

Novel Thermogravimetric Characterization Method for Adsorption Cycles of TCM

Gayaneh Issayan^{1,*}, Bernhard Zettl¹

¹ University of Applied Sciences Upper Austria, Energy Research Group ASIC, Stelzhamerstrasse 23, Wels, Austria

*Corresponding author. Email: Gayaneh.Issayan@fh-wels.at

Abstract—The ongoing process of thermochemical material development for improved thermal storage applications relies on flexible material characterization in terms of storage capacity, mechanical stability and cycling durability. This work purposes a time-efficient thermogravimetric method and the corresponding setup to characterize thermochemical materials in gram-scale batches. Beside validation of the method on the common sorbents, the applicability of the measurement setup and routines on self-produced composites inhabiting salt-hydrates in granular and pellet form are addressed. Further, accelerated cycling experiments are performed on the composites. The measurement method is found to be applicable for determining the sorption capacity and long-term cycling stability of thermochemical storage materials within inherent technological limits.

Keywords—*thermogravimetric characterization, adsorption, characteristic curves, salt-hydrate composites, TCM.*

1. INTRODUCTION

Pressing environmental and societal issues, such as natural resource management, CO₂ reduction in the atmosphere and ambitious international climate goals are motivating and enabling the research in renewable energy field. The utilization of solar energy effectively for heating applications in buildings and waste heat management in the industrial areas can immensely benefit from thermal energy storage (TES) technologies [1], [2]. In that context, thermochemical materials

(TCMs) based on physical and/or chemical sorption processes gained on interest [3]. The research paths are mainly focused on either repurposing existing sorbents for TES applications, e.g. zeolite molecular sieves, silica gel desiccants and salt-hydrates, or developing and tailoring novel ones, e.g. metal-organic frameworks (MOF) and diverse composites comprised of salt-hydrates and stabilizing host structures [4]–[6].

The thermal characterization on material level is commonly conducted by standard measurement techniques, such as Thermogravimetric Analysis (TGA) and Differential Scanning Calorimetry (DSC), or a combination of both namely Simultaneous Thermal Analysis (STA). The latter techniques are highly time-consuming and complex procedures [7]. The measurements further require distinct costly equipment, experienced staff, and limit the sample size and form. In many cases, inapt equipment or even the lack of basic research infrastructure dramatically decelerate the material development progress.

As reported in [8], salt-hydrate containing composites are developed considering application side demands on mechanical stability, sorption quality and cycling ability of the TCMs. The accessibility of material testing infrastructure in gram-batch units, various sample forms and in a time-efficient manner has been crucial to the research advancements. In this work, the functionality and design of the developed thermogravimetric setup will be discussed based on the conducted measurements on well-investigated sorbents. Ultimately, the suitability of the setup for sorption cycling of the composite TCMs will be evaluated.

2. METHODS AND MATERIALS

In this section, the efficiency of the developed setup and characterization principle will be revealed. Further investigated sorptive materials, as well as the developed composites based on salt-hydrates will be discussed.

2.1. Thermogravimetric Setup

The standardized measurement techniques and equipment (TGA, DSC, *etc.*) are designed to thoroughly investigate the thermal material properties in milligram-scale and mainly fine milled powders. A large group of common TCMs utilized in current thermal storage demonstrations come in various forms, such as granules, coarse powders and bits [9], [10]. In order to characterize the latter sorptive materials in larger laboratory batches (tens of grams) two separate setups were designed and constructed.

Generally, thermochemical systems can be operated in ambient air with a certain moisture content and atmospheric pressure, which are referred to as open systems. Likewise, thermochemical systems that are operated in evacuated (vacuum) chambers with a regulated pressure are called closed systems [1]. Both working modes are implemented in the two separate setups. The open system is controlled by the sorbent temperature variation at constant ambient conditions. The sorption process is therefore isobaric and the chamber is suitable for high temperatures in the range of 30–250 °C. Hence, the setup will be referred as high-temperature (HT) chamber. The closed system, here referred to as vacuum (VAC) chamber, is operated by variation of two parameters. First, the sorbent temperature is controlled in a lower range of 20–150 °C, and second, the vapor pressure is controlled by the adsorbate temperature. The setup has an integrated liquid reservoir, which allows a step-less temperature conditioning and the use of various adsorbates, namely water, ethanol, methanol *etc.*, and the chamber is fairly versatile. Both chambers can be operated simultaneously to cover a broad data range, as well as, each chamber can be seen as a stand-alone setup.

A schematic overview of the setups, both HT and VAC, is presented in **Figure 1**, where the components are displayed and named in detail. Each measurement setup contains a weighing cell, heater, temperature and humidity sensors. In addition, the VAC chamber is equipped with a vacuum control and temperature controlled adsorbate reservoir. The temperature control unit for both setups, as well as the data acquisition are also depicted in **Figure 1**.

The measurements in VAC chamber were mainly performed in two ways: dynamic ramps or static steps, which are shown in **Figure 2**. Dynamic ramps are the simultaneous stepwise variation of sorbent temperature with the vapor pressure. The adsorbate temperature ramp for a desorption flank, depicted in **Figure 2**, is varied from 10–0 °C, covering the corresponding pressure range of 12–6 mbar. During static desorption steps, the adsorbate temperature is kept constant, while the sorbent temperature is increased gradually. The temperatures of the steps were chosen to be 10, 5, 0 °C corresponding to 12, 9, 6 mbar. The measurement routines and their influence on the sorption capacity will be addressed in following Section 3.

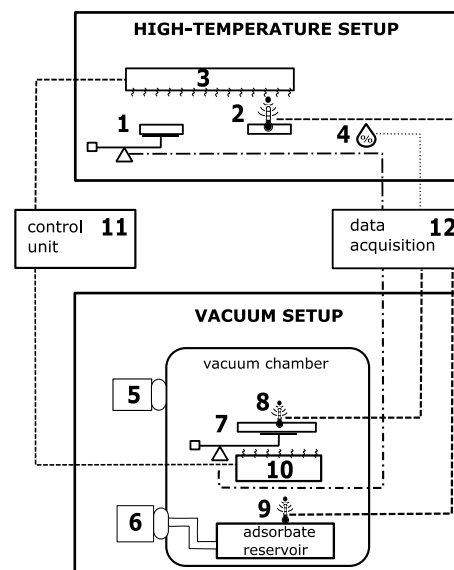


Figure 1 Schematic of the measurement setup: HT chamber consisting of (1) weighing cell and specimen crucible, (2) sorbent temp. sensor and reference crucible, (3) heater cells, (4) humidity sensor; VAC chamber consisting of (5) vacuum controller, (6) adsorbate temp. controller, (7) weighing cell and specimen crucible, (8) sorbent temp. sensors, (9) adsorbate temp. sensor, (10) heater cell, (11) temperature control unit, (12) data logger for HT and VAC chamber.

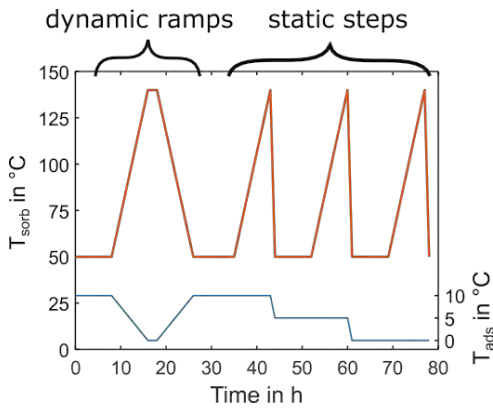


Figure 2 Two measurement routines in VAC chamber: dynamic ramps with both sorbent (top orange) and adsorbate (bottom blue) temperatures varied and static steps with constant adsorbate temperature.

2.2. Evaluation Background

Dubinin’s adsorption potential is introduced as a method for evaluating the sorption capacity of materials with various pore sizes and structures, such as activated carbons, zeolites, silica gels [11]. The adsorption potential ΔF of a sorbent to bind the adsorbate molecules as a function of sorbents temperature T_{sorb} , corresponding saturation vapor pressure p_s , vapors partial pressure in the reaction cavity p_x and the universal gas constant R is presented in Equation (1)

$$\Delta F = R \cdot T_{sorb} \cdot \ln \frac{p_s}{p_x} \quad (1)$$

Equation (2) shows the relation of the adsorption potential (Gibbs enthalpy, Gibbs or free energy, F) to the amount of the adsorbate (also water-uptake or loading, W in cm^3/g or C in g/g) at equilibrium states. The visualization of this relation is known as characteristic curve for sorbent-adsorbate pair [12]. At any given temperature and vapor pressure, there is one well- defined water-uptake value if the equilibrium state is reached. In Equation (2) the parameter W_0 stands for the maximum (saturation) water-uptake, n and E are the order of data distribution and adsorption energy between the sorbent-adsorbate pair respectively

$$W = W_0 \cdot \exp(-(\Delta F/E)^n) \quad (2)$$

The latter three parameters are usually used to fit the measurement data of mentioned common sorbents. The implementation of Dubinin’s adsorption potential and further analytical expressions (Dubinin-Astakhov) in form of characteristic curve can already be found in the literature for several material types, such as MOFs

[5], aluminophosphates (SAPO) [4], salt-based composites [6].

Thermal energy storages based on solid adsorption and/or chemical reaction can be exploited in various scenarios, such as building integrated seasonal heat generation, industrial waste heat management, surplus heat and electricity management of power plants [10]. In order to develop, compare and tune TCM-properties according to relevant technological boundaries, the necessity of defining relevant temperature and pressure levels arose. As the main interest of our research group lays in compact seasonal thermal storages for residential building applications, certain assumptions were made to set realistic measurement boundary conditions. Depending on the solar thermal installation, the upper limit for desorption can be assumed between 140–180 °C and 12 mbar for high radiation and humid summer days. The adsorption defined the lower limit of 40 °C and 6–12 mbar for winter days. The ideal case of adsorbing the material by the ambient air, which is rather dry in winter 6 mbar, as well as preconditioned air with 12 mbar was considered. The assumptions are visualized in **Figure 3** taking into account the working temperature ranges of each setup. The VAC setup is represented by the blue box with both dashed and solid lines for the mentioned worst and best pressure cases. The lower adsorption to lower desorption limit, corresponding to 300–1200 J/g are covered by data from VAC setup. The HT setup shown as orange dotted box covers the higher desorption temperatures and corresponding Gibbs energy range of 1200–1600 J/g.

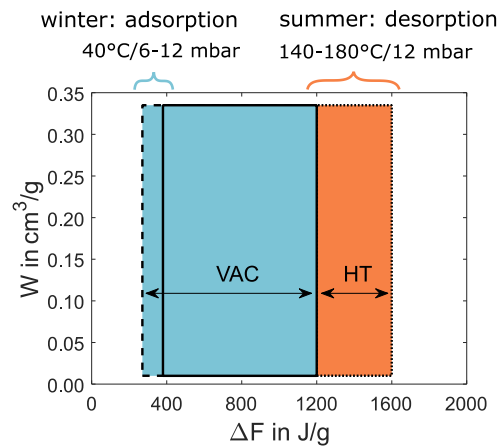


Figure 3 Storage application boundaries for data evaluation: lower boundary range for adsorption in winter 40 °C/6–12 mbar and upper boundary range for desorption in summer 140–180 °C/12 mbar.

2.3. Thermal Storage Materials

The materials examined in this work can be categorized in commercially available porous sorbents and salt-containing TCMs. The sorbents were selected based on the available data in the literature considering their utilization in the context of thermochemical storage applications. Following products will be addressed in the scope of this work: zeolites 4A binder-free (BF) and 13XBF purchased from Chemie Werke Bad Köstritz (CWK), Germany, and silica gel from Oker Chemie, Germany.

The in-house salt-hydrate composites were produced as reported in [8] using natural zeolite clinoptilolite and phyllosilicate vermiculite as different pore-sized hosts. Lithium and calcium chlorides were both used in different weight ratios. The raw materials were then processed to granules or pellets with hydraulic binders, which can be observed in optical microscopy images of two exemplary composites in **Figure 4a** and **4b**. The relevant composition of the presented compounds will be disclosed in Section 3, where the notation for sample composition follows the scheme: [binder-type][binder-content]-[salt-content]-[host material] (shape). For example the sample PS3-40-V(G) contains:

- 3 wt.% Portland and sulfate additive mixture
- 40 wt.% salt-hydrate content
- Remaining 57 wt.% vermiculite
- Spherical granules

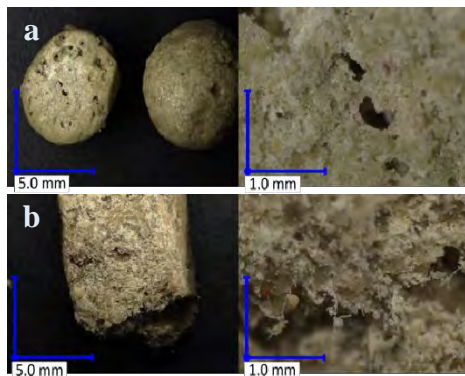


Figure 4 Optical microscopy images: (a) composite sample PS3-40-C(G) in spherical granular form and (b) composite sample PS20-40-C(P) in compact cylindrical pellet form.

As the focus of this paper lays in the utilization of the thermogravimetric setup, rather than the thermochemical materials themselves, a variety of measurements will be presented and discussed disregarding the specific composite qualities. For demonstration purposes, composites with similar salt-

hydrate content of about 40–45 wt.% are selected for the discussion of the results on larger composites. The sizes of presented composites in granule form range from 4–8 mm in diameter and pellet-formed samples have diameters of roughly 5–10 mm and heights up to 15 mm.

3. RESULTS

In this chapter, the functionality and reliability of the measurement setup will be verified based on published material data from the literature. Additionally, suitable measurement routines and set parameter for sorption cycles will be deployed to ensure reproducible results. Following the validation, the results of salt-containing composites of different compositions will be presented. Finally, the met challenges, proposed solutions and interpretations of the results will be discussed.

3.1. Validation

The adsorption process depends on the mass and heat transport rates within the sample. Those can be improved by increasing the surface area of the sample to enhance solid–gas interaction, which poses as a problem in case of larger grains in TGA measurements. Further, the equipment is designed for only small sample portions in the range of 50–75 mg, which also leads to the investigation of only a few grains at once. The named equipment is highly sensitive to setting movements and disturbances during the measurements of larger grains and the results may not fully reflect the material behavior in loose bed. The adequate measurement of mass change caused by adsorption of the gaseous phase is conducted by establishing a thermodynamic equilibrium state of the sorption process at a particular temperature and partial pressure. After the mass signal is stabilized for a certain period of time (hours) a single data point of the isotherm is registered. Hence, the procedure is time-consuming considering the quantity of the resulting data.

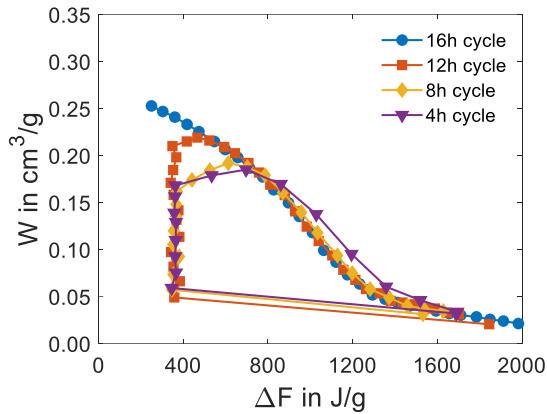


Figure 5 Adsorption cycles of 4ABF zeolite at different temperature variation rates in HT setup. The cycles with 16 (blue circles) and 12 hours (orange squares) overlap in contrast to 8 (yellow rhombus) and 4 hour (purple triangle) cycles [13].

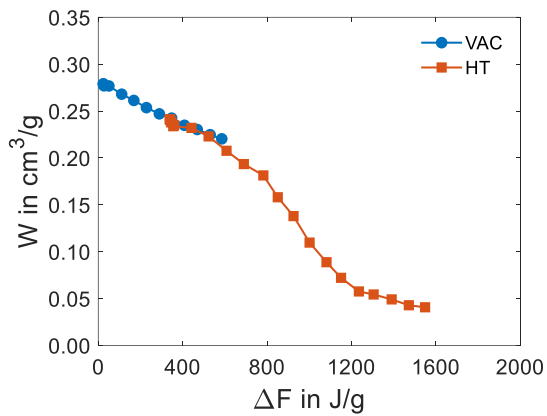


Figure 6 4ABF zeolite adsorption data from both VAC (blue circles) and HT (orange squares) chamber [13].

The purposed measurement routine depends on the determination of the sufficient temperature variation rate to reach the consecutive equilibrium states. The measurements on zeolites were performed using the dynamic ramp regime. The results of four cycles in HT chamber are depicted in **Figure 5**, where the cycle duration is decreased. The first two cycles with 16 and 12 hours overlap, indicating properly achieved adsorption states, in contrast to the strongly deviating cycles with 8 and 4 hours. It is worth mentioning, that the materials adsorption/desorption cycle duration should be also selected realistically and considered in the application design.

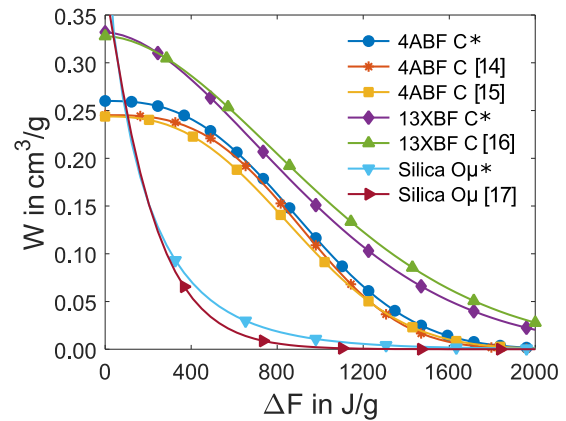


Figure 7 Fitted characteristic curves of 4ABF, 13XBF zeolites (CWK) and micro-porous silica gel (Oker) marked by *star [13] in comparison with literature data [14]-[17].

Two sample batches of the same material with the same initial conditions were measured simultaneously in both VAC and HT chambers, and the resulting characteristic curves are displayed in **Figure 6**. The two sets of data overlap sufficiently, which indicates the legitimacy of the conducted measurements. The data was then fitted following Equation (2) and the parameter can be further processed to generate arbitrary isotherms, isobars and isosters.

In order to compare the results from the developed setup and data available in literature fitted characteristic curves of zeolites 4ABF, 13XBF and silica gels are presented in **Figure 7**. The measurement results are in agreement with the literature, which validates the measurement principle and functionality of the setup for samples exhibiting solely physisorption.

3.2. Salt-Hydrate Containing Composites

The adsorption/hydration behavior of salt-containing composites is assumed to be a complex and multilateral process, due to the number of interacting and cascading mechanisms like solid sorption of the host matrix, hydration of salts and bedding structure of inactive binder [8], [18]. Dominant influencing factors beside the content of active vs. inactive materials, are mass and heat transport through the sample, as well as processing parameters, such as pore size distribution, density and geometry. Additionally, due to the strong hygroscopic character of calcium chloride, deliquescence humidity limits, agglomeration and overhydration of the composites at low temperatures and high pressures had to be controlled. Therefore, further measurements were performed to determine, if

salt-containing composites can be adequately characterized by the purposed method. The latter one allows a continuous scan of a large temperature and pressure (Gibbs energy) range generating a substantial amount of data points to thoroughly observe typical hydration behavior (steps) of the salt-hydrates.

Cycling experiments with varying temperature rates were performed as described in Section 3.1. Nevertheless, for a comprehensive interpretation of the results the static approach at constant 8 mbar vapor pressure in VAC chamber was selected. Adsorption cycles of the sample PS15-40-C(G) in both VAC and HT setups are presented in **Figure 8**. In both cases the cycles with 4 (blue circles) and 8 hours (orange stars) duration show insufficient adsorption/hydration of the sample. Yet, the cycles with 16 (yellow rhombus) and 24 hours (purple squares) overlap, indicating adequate water-uptake. The difference in the adsorption levels during the cycles for the latter cases is practically indistinguishable. Further, in case of the 8 hour cycle in VAC setup the difference is rather neglectable. The relevant gain in water-uptake is in the range of 400–1000 J/g. Therefore, further discussions regarding composites will only address the measurements from VAC chamber.

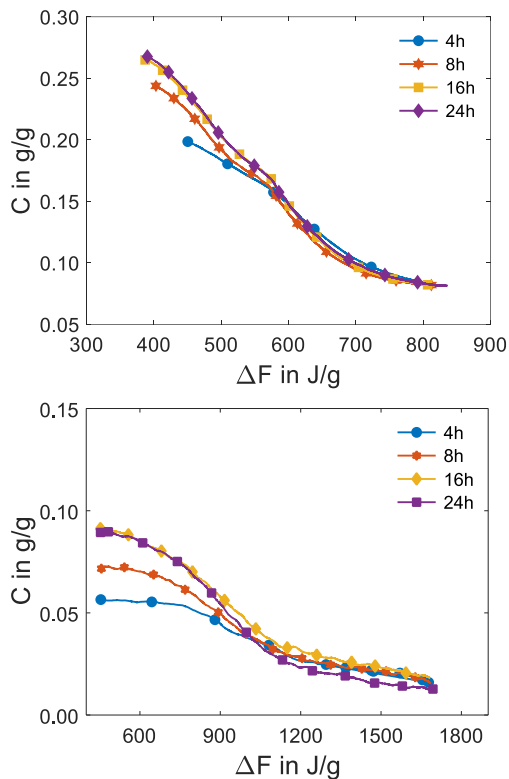


Figure 8 Adsorption cycles of PS15-40-C(G) at different temperature variation rates in (top) VAC

and (bottom) HT setup. In both cases the cycles with 4 (blue circles) and 8 hours (orange stars) duration are not sufficient and cycles with 16 (yellow rhombus) and 24 hours (purple squares) overlap, indicating an adequate adsorption/hydration.

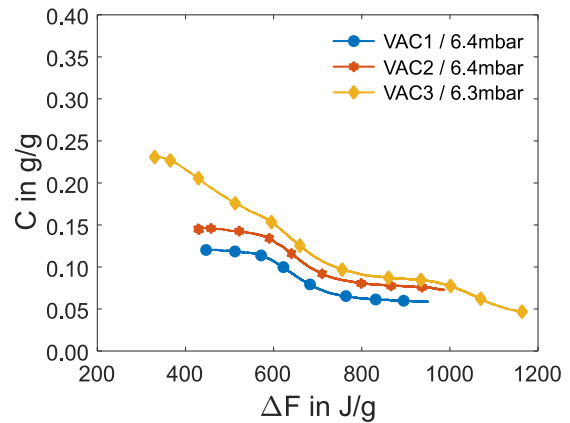


Figure 9 VAC measurements cycles with variations of the sorption temperature range and initial loading on PS10-45-V(P).

The next step was to observe the influence of temperature variation in a cycling experiment. The data displayed in **Figure 9** presents three measurement cycles of PS10-45-V(P) at comparable pressures around 6.4 mbar. For the initial cycle (blue circles) the sample was dried by flushing with dry pressurized air at 250 °C. In comparison to the not fully dried sample in the second cycle (orange stars), the data from the first shows poor adsorption/hydration within the same narrow temperature range of 50–100 °C. The contrast is more significant in the case of the third cycle, where the temperature range is broader from 40 to 130 °C. The results point out the importance of sufficient adsorption and desorption temperature level to fully employ the potential of the salt-hydrates in the composites. Within the storage application, where the temperature levels cannot be provided, the cycle duration should be increased accordingly. In this context, the importance of the state of the charge

determination for controlled utilization of TCM in applications can be mentioned.

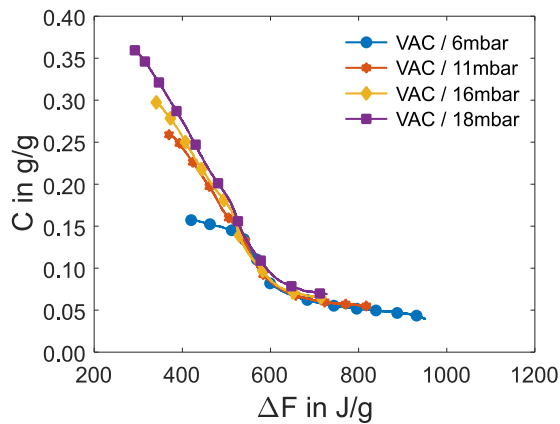


Figure 10 VAC measurement cycles with partial pressure variations in the chamber on PS15-40-C(G).

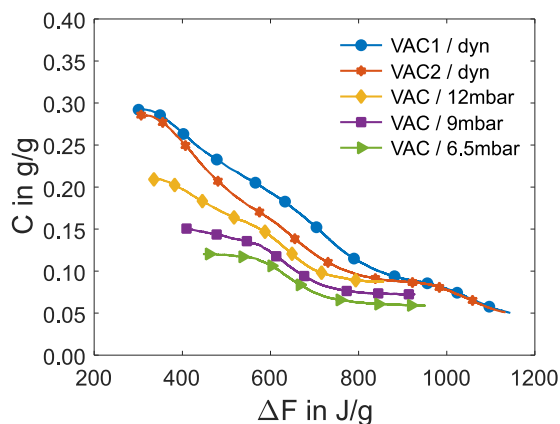


Figure 11 Static and dynamic measurements on PS10-45-V(P).

Additionally, the measurements comparing the cycles with increasing vapor pressures in **Figure 10** also indicate a preferable operation scope for the composite samples. As expected, the lowest sorption capacity of PS15-40-C(G) is observed at 6 mbar pressure (blue circles), which then increases steadily with pressure. In the narrow Gibbs energy range between 300– 600 J/g the composites demonstrate a water-uptake up to 30 wt.%.

As the significance of pressure increase was addressed, the last step towards accelerated cycling experiments with the intended setup and measurement routine was to perform dynamic measurements. **Figure 11** displays successive cycles on PS10-45-V(P) with a stepwise increasing pressures, where the

evolution of the sorption capacity can be observed, followed by two dynamic cycles. The latter data was collected by overall pressure variation between 7– 9 mbar. The trend and succession of the dynamic characteristic curves display a consistent shape compatible to the static curves. Nevertheless, the dynamic cycles outperform the static ones regarding sorption capacity. This phenomenon will be the topic of further investigations and will be addressed again in cycling results.

3.3. Accelerated Cycling of Composites

The final and most crucial part of this work contains the experimental results of two accelerated long-term cycling measurements. The selected composites strongly differ in salt-content and form. In addition, the cycling regimes differ in the implementation method and temperature range. First results belong to a sample with a high salt-content PS10-45-C(P) in larger pellet forms, which was cycled 20 times at high adsorption and desorption temperatures of about 60 and 150 °C. This material was cycled in a static pressure regime at 9 mbar. The raw mass and temperature signals are presented in **Figure 12a** and the mass increase in reference to the dry mass for each adsorption and desorption flank is calculated and displayed in **Figure 12b**.

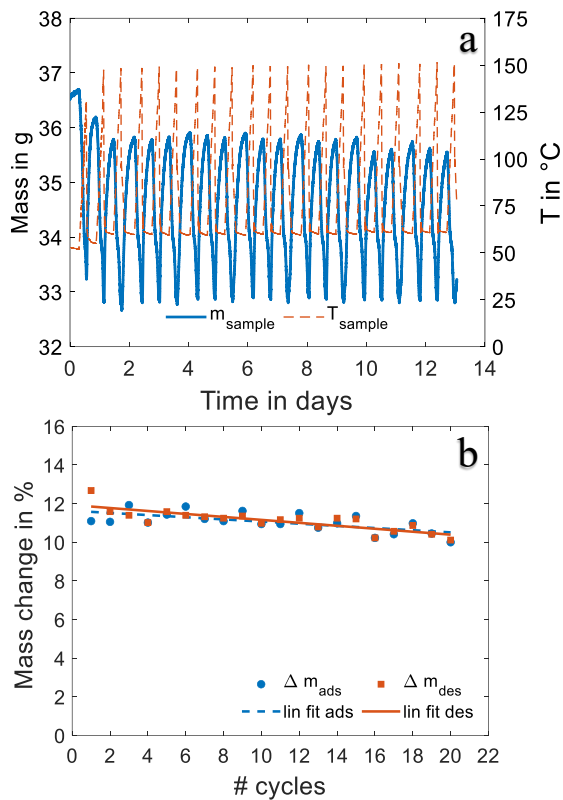


Figure 12 Example of static cycling of PS10-45-C(P): (a) raw sorbent temperature and mass cycling data, (b) percentile masschange for ad-/desorption slopes of every cycle.

The sorption capacity of the high salt-content sample is estimated to be roughly around 12% and is rather low even during the first cycles and the losses upon cycling yield 2% over 20 cycles.

The set of results presented in **Figure 13a** and **13b** refer to the sample PC5-20-C(G) with low salt-hydrate weight ratio, yet smaller granule size around 3–4 mm. The chosen temperature range was set between 30 and 125 °C, which is lower than in **Figure 12a**. Beside the geometrically preferable spherical shape and small diameter, the main difference here is the use of dynamic cycling routine with a pressure span of 7–9 mbar instead of a constant pressure level. The water-uptake results of the dynamic cycling experiment are significantly higher despite the low salt-content of the sample. The overall sorption capacity over the cycles can be estimated to 26–27% with 0.5–1.0% losses over 16 cycles. The adsorption flanks show an overall higher loss than desorption data, which can be observed by the slope of the linear fit. Despite the high standard deviation of the data, the granules perform well upon cycling in comparison to the static cycled pellets.

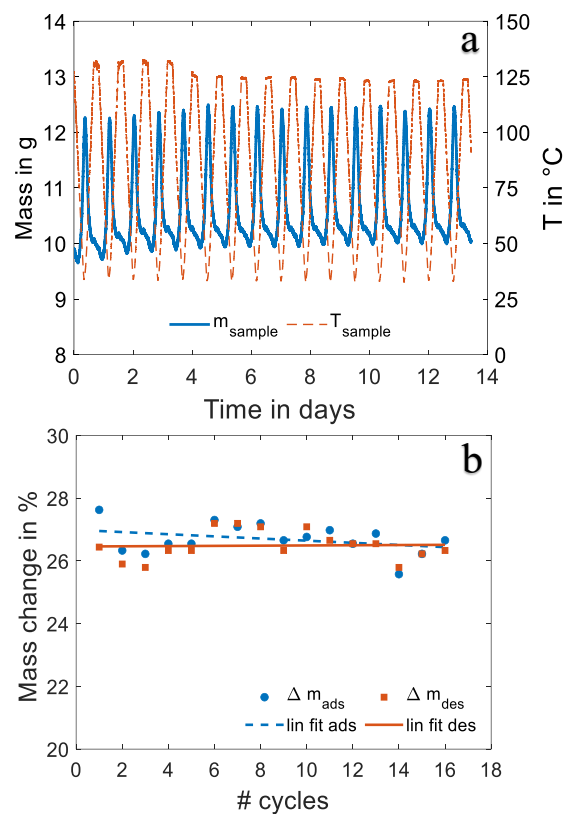


Figure 13 Example of dynamic cycling of PC5-20-C(G): (a) raw sorbent temperature and mass cycling data, (b) percentile masschange for ad-/desorption slopes of every cycle.

4. CONCLUSION

In this work, a thermogravimetric setup and corresponding measurement routines are introduced for a time-efficient characterization of thermochemical materials in a broad temperature range. The setup consists of two separate chambers representing the open and closed adsorption systems, high-temperature and vacuum chamber, respectively. Both chambers are comprised of low-cost components and do not rely on complex control regimes. Therefore, they can be readily replicated with frequent laboratory equipment. The setup is designed for up to tens of grams of solid sample batches with no limitations on shape or form of the material. Further, the measurement duration (cycling time) as a hindering factor is tackled by this method. The mass signal is recorded continuously and generates a comprehensive scan over a broad span of temperature and humidity values.

The introduced measurement method using characteristic curve as visualization is validated based on well-studied 4A, 13X zeolites and microporous

silica gel. Further, measurements on salt-hydrate containing composites demonstrate adequate adaptability of the method. The influence of substantial parameter variation is demonstrated on various composites. The partial pressure variation was approached in two ways, first by keeping the pressure at constant levels (static), and second by dynamically varying it together with sorbent temperature. The results of dynamic measurements outperform the static ones at equal pressures. The dynamic routine should be further investigated and reproduced for salt-containing composites. Additionally, the applicability of the dynamic method should be evaluated in the scope of technological realization on storage level to elicit the potential of the composites.

The measurement method allows fast ad-/desorption cycles, which was utilized in accelerated cycling experiments testing the stability of the composites in simulated conditions of seasonal thermal storage (one cycle per year). The advantages of low adsorption temperature and the dynamic pressure variation are demonstrated in terms of significant higher sorption capacity of the granulated samples. The results of dynamic cycling experiments are promising and will be the topic of further examinations.

ACKNOWLEDGMENTS

The authors gratefully acknowledge the financial support for project New-TCM (Wi-2018-97351-/9-RA) by the EU-European Regional Development Fund (ERDF) and Federal Province of Upper Austria-Investments in Growth and Jobs (IGJ).

REFERENCES

- [1] J. Lizana, R. Chacartegui, A. Barrios-Padura, C. Ortiz, Advanced low-carbon energy measures based on thermal energy storage in buildings: A review, in: *Renewable and Sustainable Energy Reviews*, 2018, vol. 82, pp. 3705–3749.
- [2] L. Miró, J. Gasia, L. F. Cabeza, Thermal energy storage (TES) for industrial waste heat (IWH) recovery: A review, in: *Applied Energy*, 2016, vol. 179, pp. 284–301.
- [3] L. Scapino, H. A. Zondag, J. Van Bael, J. Diriken, C. C. Rindt, Sorption heat storage for long-term low-temperature applications: A review on the advancements at material and prototype scale, in: *Applied Energy*, 2017, vol. 190, pp. 920–948.
- [4] S. K. Henninger, F. Jeremias, H. Kummer, P. Schossig, H.-M. Henning, Novel sorption materials for solar heating and cooling, in: *Energy Procedia*, 2012, vol. 30, pp. 279–288.
- [5] M. Solovyeva, L. Gordeeva, T. Krieger, Y. I. Aristov, MOF-801 as a promising material for adsorption cooling: Equilibrium and dynamics of water adsorption, in: *Energy Conversion and Management*, 2018, vol. 174, pp. 356–363.
- [6] A. Ristić, N. Zabukovec Logar, New composite water sorbents CaCl₂-PHTS for low-temperature sorption heat storage: determination of structural properties, in: *Nanomaterials*, 2019, vol. 9, no. 1, p. 27.
- [7] D. Lager, Evaluation of thermophysical properties for thermal energy storage materials determining factors, prospects and limitations, Ph.D. dissertation, TU Vienna, Austria, 2017.
- [8] G. Issayan, B. Zettl, W. Somitsch, Developing and stabilizing salt-hydrate composites as thermal storage materials, in: *14th International Renewable Energy Storage Conference 2020 (IRES 2020)*. Atlantis Press, 2021, pp. 49–57.
- [9] B. Zettl, G. Englmaier, G. Steinmaurer, Development of a revolving drum reactor for open-sorption heat storage processes, in: *Applied Thermal Engineering*, 2014, vol. 70, no. 1, pp. 42–49.
- [10] H. Jarimi, D. Aydın, Z. Yanan, G. Ozankaya, X. Chen, S. Riffat, Review on the recent progress of thermochemical materials and processes for solar thermal energy storage and industrial waste heat recovery, in: *International Journal of Low-Carbon Technologies*, 2019, vol. 14, no. 1, pp. 44–69.
- [11] M. Dubinin, The potential theory of adsorption of gases and vapors for adsorbents with energetically nonuniform surfaces, in: *Chemical Reviews*, 1960, vol. 60, no. 2, pp. 235–241.
- [12] A. Hauer, Beurteilung fester Adsorbentien in offenen Sorptionssystemen für energetische Anwendungen, Ph.D. dissertation, TU Berlin, Germany, 2002.
- [13] B. Zettl, G. Issayan, A time-efficient characterization method for sorbents used as TES materials and its application to zeolite and salt-composite materials, 2020, submitted to *Adsorption*.
- [14] CWK Bad Köstritz GmbH, Product data sheet, provided by manufacturer.

- [15] T. H. Herzog, J. Jänchen, Adsorption properties of modified zeolites for operating range enhancement of adsorption heat pumps through the use of organic adsorptive agents, in: *Energy Procedia*, 2016, vol. 91, pp. 155– 160.
- [16] R. Weber, S. Asenbeck, H. Kerskes, R. Jaudas, *Solspaces: final report*, Institute for Thermodynamics and Thermal Engineering (ITW), Technical Report, 2016. [Online]. Available: https://www.igte.uni-stuttgart.de/veroeffentlichungen/publikationen/SolSpaces_AB_final.pdf
- [17] A. Sapienza, A. Velte, I. Girnig, A. Frazzica, G. Földner, L. Schnabel, Y. Aristov, “water-silica siogel” working pair for adsorption chillers: Adsorption equilibrium and dynamics, in: *Renewable Energy*, 2017, vol. 110, pp. 40–46.
- [18] K. Posern, K. Linnow, M. Niermann, C. Kaps, M. Steiger, Thermo- chemical investigation of the water uptake behavior of MgSO₄ hydrates in host materials with different pore size, in: *Thermochimica Acta*, 2015, vol. 611, pp. 1–9.